Evolution of T^2 resistivity and superconductivity in Nb_3Sn under pressure

Z. Ren,[1,2,*] L. Gamperle,[1] A. Fete,[1] C. Senatore,[1] and D. Jaccard[1]

[1]*DQMP - University of Geneva, 24 Quai Ernest-Ansermet, 1211 Geneva 4, Switzerland*

[2]*Institute for Natural Sciences, Westlake Institute for Advanced Study, 18 Shilongshan Road, Hangzhou, P. R. China*

(Received 26 October 2016; revised manuscript received 14 April 2017; published 1 May 2017)

We present a resistivity study of single- and polycrystalline Nb_3Sn under pressure up to 9.3 GPa. Despite quite different pressure responses, T_c of both samples is diminished with increasing pressure. Above T_c, their resistivity follows a T^2 dependence whose coefficient A decreases with pressure. We show that the bulk T_c depends linearly on $\sqrt{A}$, and the slope of this linear contribution becomes larger with the increase of disorder. Our results suggest that the density of states at the Fermi level plays an important role in governing the pressure dependence of T_c in Nb_3Sn.

DOI: 10.1103/PhysRevB.95.184503

I. INTRODUCTION

The A15 superconductor Nb_3Sn has attracted a lot of attention [1–3] because it is widely used in nuclear magnetic resonance spectroscopy [4], nuclear fusion reactions [5], and is the designed superconducting magnet material for the high luminosity upgrade of the Large Hardon Collider as well as the main candidate for future accelerators [6]. At ambient pressure, Nb_3Sn undergoes a cubic-to-tetragonal structural transition upon cooling around $T_M \sim 30$–43 K, and becomes a superconductor below $T_c \sim 18$ K [3]. Compared with element Nb, the one-dimensional arrangement of Nb atoms in Nb_3Sn results in a large and rapidly varying density of states $[N(E_F)]$ near the Fermi level [7] and consequently favors a strong electron-phonon coupling. These factors are generally believed to be responsible for the relatively high T_c [3], although pairing through electron-electron interactions was also proposed [8,9].

For high-field application of Nb_3Sn, the understanding of mechanical stress dependence of its critical superconducting parameters, such as T_c, J_c, H_{c2}, is of significant interest since the electromagnetic force grows quadratically with magnetic field [10]. Previous high-pressure studies of Nb_3Sn have shown that pressure enhances T_M while it suppresses T_c [11], whose underlying mechanism remains under debate. One possibility is that the opposite trend in the pressure derivative of T_c and T_M is mainly due to pressure-induced shift of phonon spectrum [12]. An alternative scenario is that T_c and T_M are governed by the change of d-electron number in the subband due to charge redistribution [13,14]. Actually, a similar debate exists concerning the origin of the T^2 dependence of resistivity above T_c at ambient pressure [15]. Hence, it is worth investigating the pressure evolution of the T^2 resistivity as well as its connection with T_c, which may provide useful insights into these debates.

In this paper we present a study of the high-pressure resistivity of Nb_3Sn up to ~9 GPa on a single-crystalline and a polycrystalline sample with extrapolated residual resistivities ~1 and ~9 $\mu\Omega$ cm, respectively. Superconductivity in the polycrystalline sample is weakened more rapidly under pressure than in the single-crystalline one. In the normal state, the resistivity of both samples follows a AT^2 dependence in the whole pressure range investigated. Remarkably, the depression of the bulk T_c is found to be a linear function of $\sqrt{A}$. Furthermore, $dT_c^{bulk}/d\sqrt{A}$ increases with ρ_0. The implication of these results on the pairing mechanism in Nb_3Sn is also discussed.

II. EXPERIMENT

The polycrystalline Nb_3Sn sample was prepared by reacting high-purity elements in a HIP (hot isostatic pressure) furnace at 200 MPa and 1250 °C for 24 h followed by cooling at a rate of 30 °C per hour to 0 °C [16], hereafter referred to as Nb_3Sn(P). Tiny Nb_3Sn crystals with dimensions of several hundred micrometers were grown by the iodine vapor transport method and screened by magnetic susceptibility measurements, hereafter referred to as Nb_3Sn(S). To better determine the resistivity magnitude of Nb_3Sn(S), we have measured multiple samples to get a mean resistivity value at room temperature for normalization. The errors in the resistivity value are estimated to be 5% and 1.5% for Nb_3Sn(S) and Nb_3Sn(P), respectively. At ambient pressure, the temperature dependencies of resistivity of the samples were measured in cryostats under magnetic fields of 0 and 19 T parallel to the current direction. High-pressure experiments were performed using a Bridgman-type WC (tungsten carbide)-anvil cell with steatite as the soft-solid pressure medium and lead (Pb) as the pressure gauge [17]. The resistivity was measured by using a standard four-probe method and for Nb_3Sn(S), the applied current is along the [100] axis. The pressure gradient along the sample, as estimated by the superconducting transition of a Pb manometer, slowly increases from 0.3 GPa at initial pressure up to 0.5 GPa at maximum pressure. At 292 K, high pressure isothermal resistivity was extrapolated to $p = 0$ and the obtained value was normalized to the one measured at ambient condition, yielding an effective form factor for the pressurized sample. This factor can be considered as pressure independent within 5%, which was confirmed after depressurization.

III. RESULTS AND DISCUSSION

A. Ambient pressure results

Figure 1(a) shows the temperature dependence of the resistivity (ρ) for Nb_3Sn(S) and Nb_3Sn(P) at ambient pressure. For both samples, the normal-state ρ exhibits a pronounced curvature, consistently with [18]. Notably, the data of Nb_3Sn(P)

*zhi.ren@wias.org.cn

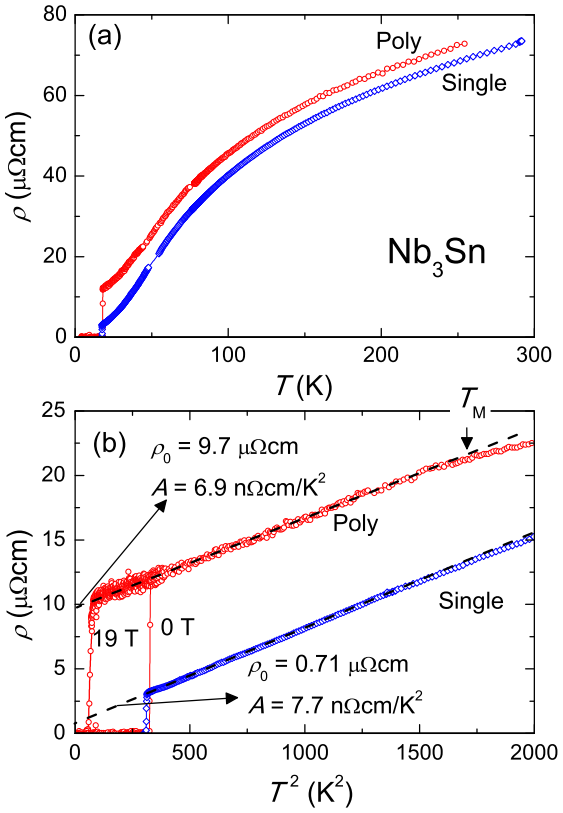

FIG. 1. (a) Temperature dependencies of resistivity of Nb_3Sn(S) and Nb_3Sn(P) at ambient pressure. (b) Low-temperature region of the data plotted as a function of T^2. The result of Nb_3Sn(P) at 19 T is also included. The dashed lines are a guide to the eyes. The structural phase transition temperature T_M is marked by the arrow.

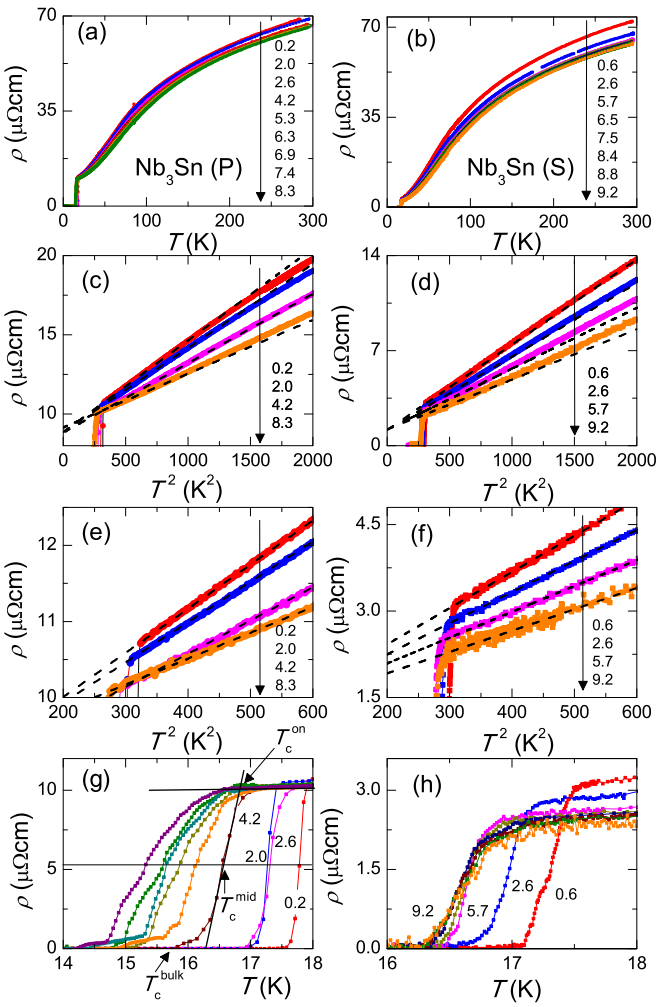

FIG. 2. (a) and (b) The temperature dependencies of resistivity under various pressure for Nb_3Sn(P) and Nb_3Sn(S), respectively. (c) and (d) The low-temperature resistivity plotted as a function of T^2 at selected pressures for the two samples. The dashed lines are linear fits to the data below 600 K^2. (e) and (f) The zooms of (c) and (d) just above T_c. The dashed lines are the same as those in (c) and (d). (g) and (h) The superconducting transition under pressure for the two samples. See text for the definition of T_c^{on}, T_c^{mid}, and T_c^{bulk}.

is an almost rigid upward shift of that of Nb_3Sn(S), indicating that the temperature-dependent electron scattering mechanism does not depend on the sample nature. Hence the difference in the resistivities of the two samples mainly corresponds to different degrees of disorder.

As shown in Fig. 1(b), in both cases, the $\rho(T)$ data from T_c up to ~35 K can be well described by the relation $\rho(T) = \rho_0 + AT^2$, where ρ_0 is the residual resistivity and A is the prefactor. Upon application of a 19-T magnetic field, this T^2 law extends down to ~10 K for Nb_3Sn(P), while this is not the case in Nb_3Sn(S) due to a non-negligible positive magnetoresistance (data not shown). With increasing temperature above ~35 K, $\rho(T)$ shows a downward deviation from the T^2 behavior, although the anomaly due to the structural phase transition is more visible in Nb_3Sn(P). In addition, in spite of its slightly higher T_c, ρ_0 of Nb_3Sn(P) is nearly one order of magnitude higher than that of Nb_3Sn(S). It is known that ρ_0 of the Nb-Sn system is sensitive to the atomic Sn content, with a reduction by one order of magnitude between 24 and 25 at. % observed in both homogenous bulk samples and single crystals [19]. This suggests the presence of a Sn concentration distribution within the Nb_3Sn(P) sample.

B. Electrical resistivity under pressure

Figure 2 shows the resistivity of Nb_3Sn(S) and Nb_3Sn(P) under pressure up to ~9 GPa. We note the following similarities between the two samples. First, the shape of $\rho(T)$ remains nearly unchanged while its magnitude decreases slightly with increasing pressure. Second, when plotted against T^2, a linear region in $\rho(T)$ can always be found with its slope decreasing with increasing pressure. Although weak, it seems clear that above a certain temperature (~25–35 K) $\rho(T)$ exhibits a downward deviation at low pressure but an upward deviation at high pressure from the T^2 dependence, suggesting the presence of additional contributions from the structural transition and the conventional electron-phonon scattering to the resistivity. Nevertheless, as shown clearly in Figs. 2(e) and 2(f), the T^2 law appears to provide a good description of all the data above T_c [20]. Yet, it remains to be seen whether the normal-state

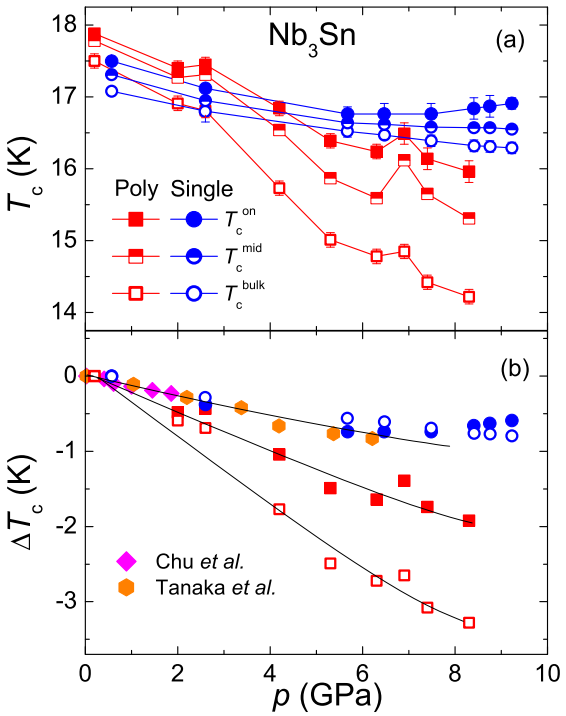

FIG. 3. (a) Pressure dependencies of the temperatures corresponding to the onset (T_c^{on}), the midpoint (T_c^{mid}), and the completion (T_c^{bulk}) of the resistive superconducting transition for Nb_3Sn(S) and Nb_3Sn(P). (b) $\Delta T_c = T_c(p) - T_c(0)$ plotted as function of pressure. The results from Refs. [11,21] are also included for comparison. The solid lines are a guide to the eyes.

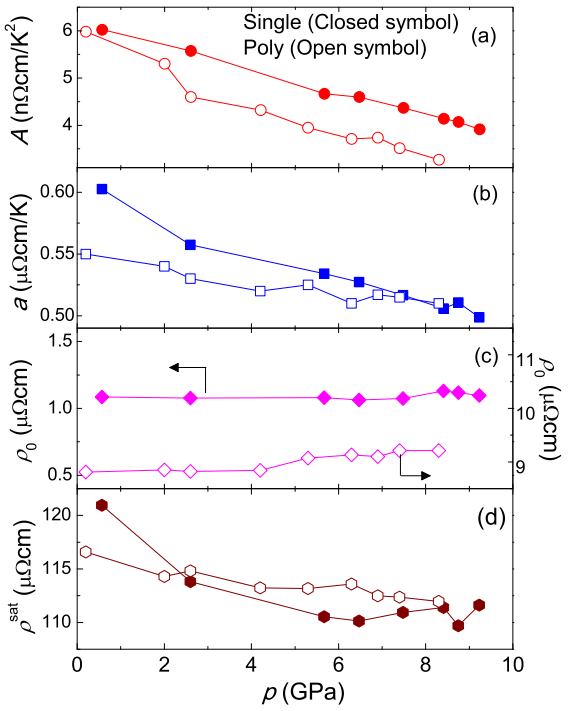

FIG. 4. Pressure dependencies of the coefficients A, a, residual resistivity ρ_0, and saturation resistivity ρ^{max} derived from the data fitting for Nb_3Sn(S) (closed symbol) and Nb_3Sn(P) (open symbol).

resistivity follows a T^2 law down to zero temperature by combining high pressure and high magnetic field. Third, T_c tends to decrease and the superconducting transition becomes broadened with pressure.

Let us now examine the pressure dependence of T_c. It is noted that additional steplike features show up in the superconducting transition at some pressures, which is ascribed to the pressure inhomogeneity in the pressure cell. Hence, for each pressure, we determine T_c^{on} as the temperature corresponding to the intersection of a linear extrapolation of the initial resistivity drop with the normal-state line, T_c^{mid} as the temperature corresponding to the midpoint of the resistivity transition, and T_c^{bulk} as the temperature corresponding to the completion of the resistive transition, which coincides usually with the midpoint of the jump in ac heat capacity (see Appendix). As shown in Fig. 3(a), with increasing pressure, the depression of T_c and the increase in the transition width are more rapid for Nb_3Sn(P) than for Nb_3Sn(S). In order to allow for a straightforward comparison, we plot in Fig. 3(b) $\Delta T_c = T_c(p) - T_c(0)$ as a function of p for the two samples together with the data reported by Chu *et al.* [11] and Tanaka *et al.* [21]. ΔT_c^{on} of Nb_3Sn(S) is less than 1 K up to 9.3 GPa, in good agreement with previous reports [11,21]. By contrast, ΔT_c^{on} and ΔT_c^{bulk} of Nb_3Sn(P) increase to ~2 and ~3 K, respectively. Here it should be pointed out that the pressure gradient is very similar for the two pressure cells. Hence the strong sample dependence of $\Delta T_c(p)$ is most probably of intrinsic origin, as found earlier in [22].

We now turn our attention to temperature behavior of the normal-state resistivity. As shown above, the low-T data is well described by a T^2 law. On the other hand, the $\rho(T)$ data above 200 K can be fitted using a parallel-resistor model $1/\rho(T) = 1/(\rho_0 + aT) + 1/\rho^{max}$, where a is the coefficient due to electron-phonon scattering and ρ^{max} is the saturation resistivity [18]. The obtained parameters for Nb_3Sn(S) and Nb_3Sn(P) are shown in Fig. 4, and display a qualitatively very similar pressure dependence. As can be seen, ρ_0 remains essentially unchanged, suggesting that pressure does not introduce much additional disorder. Unlike ρ_0, all the other parameters decrease with pressure. Since $a \sim 1/\Theta_D^2 \sim V^{2/3}$ and $\rho^{max} \sim V^{1/3}$, where Θ_D is the Debye temperature and V is the unit cell volume, the decrease of these parameters can be understood as resulting from the shrinkage of V under pressure.

Surprisingly, both the A coefficient and ρ_0 show discontinuity between the ambient and first measured pressure, although T_c is smooth as well as a and ρ^{max} values. These sudden changes can be tentatively ascribed to strain effect in the soft solid transmitting pressure medium [10,23]. Strain is expected to abruptly grow during the initial pressurization and slowly increase with further increasing pressure, similar to the pressure gradient. Likely, the strain field has the pressure chamber axial symmetry which was chosen to coincide with the [110] axis of Nb_3Sn(S). Thus subtle interplay between volume contraction and strain effects have to be detailed in the future. Consistently strain effect appears to be stronger in single than in polycrystalline Nb_3Sn. In addition, the small increase in ρ_0 of Nb_3Sn(S) could be due to pressure-induced dislocations or even micro cracks.

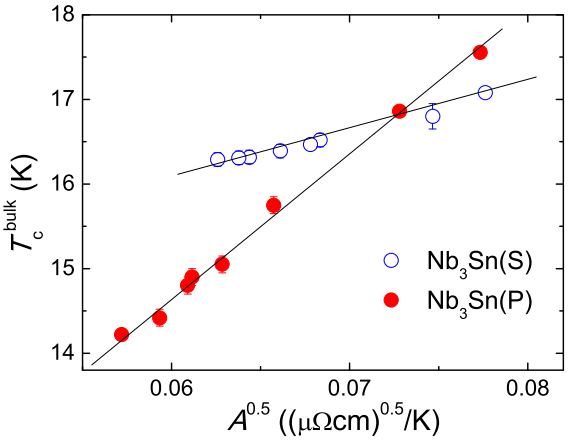

FIG. 5. T_c^{bulk} plotted as a function of $\sqrt{A}$ for Nb_3Sn(S) and Nb_3Sn(P) under pressure. The solid lines are a guide to the eyes.

Given that there is still some debate on the origin of the T^2 resistivity in Nb_3Sn, the pressure evolution of the A coefficient deserves scrutiny. According to Webb *et al.*, the T^2 dependence could be due to phonon assisted s-d interband scattering with a spectrum $F(\omega)$ of non-Debye-like phonons [15]. However, Gurvitch *et al.* later found that even in highly disordered Nb_3Sn, whose phonon spectrum is apparently different from the crystalline one, this T^2 dependence of the resistivity is still observed [24]. Furthermore, more elaborated calculations by Caton and Viswanathan shows that only a T^3 dependence of the resistivity can arise due to the phonons in V_3Si, yet its low-temperature resistivity follows the T^2 law [25]. It thus appears that the T^2 dependence of the resistivity has little to do with the phonon structure.

In fact, our results are more in line with the electron-electron scattering scenario [26]. In this second scenario, since $A \propto [N(E_F)]^2$ and $N(E_F)$ is large in Nb_3Sn, the large A values (~6–7 $n\Omega$ cm/K^2) gets a natural explanation. Moreover, its decrease under pressure is in agreement with the reduction of $N(E_F)$ as suggested by previous experimental [14] and theoretical studies [27,28].

The concomitant decrease of T_c and A with pressure is reminiscent of what has been observed in V_3Si [29], Sr_2RuO_4 [30], heavy fermion compounds [31,32], and borocarbides [33,34], and points to a close relationship between these quantities. Actually, as shown in Fig. 5, when plotting T_c^{bulk} against $\sqrt{A}$, a linear behavior is observed in both cases, meaning that $dT_c^{bulk}/d\sqrt{A} \propto dT_c^{bulk}/dN(E_F)$ remains unchanged under pressure. It thus appears that $N(E_F)$ is the key factor in determining the pressure dependence of T_c^{bulk} for a given sample. This result is consistent with a previous study which shows that for Nb_3Sn T_c is a function mainly of $N(E_F)$ [35]. In addition, $dT_c^{bulk}/d\sqrt{A}$ of Nb_3Sn(P) is nearly three times that of Nb_3Sn(S), suggesting that disorder also plays a role in determining T_c. This is understandable since $N(E_F)$ and ρ_0 are related [36].

C. Implication on the pairing mechanism

Nb_3Sn is generally considered as a BCS superconductor with a strong electron-phonon coupling [3]. For this kind of superconductors, T_c can be estimated from the McMillan formula [37] $T_c = (\Theta_D/1.45)\exp\{-[1.04(1+\lambda)]/[\lambda - \mu^*(1+0.62\lambda)]\}$, with $\lambda = [N(E_F)\langle I^2\rangle/M\langle\omega^2\rangle]$, where μ^* is the Coulomb pseudopotential, $\langle I^2\rangle$ is the average square electron-ion matric element, M is the atomic mass, and $\langle\omega^2\rangle$ is the average square phonon frequency. Indeed, with a λ value of 1.51 from first-principles calculations [38] and $\mu^* = 0.15$, the predicted T_c of 17.7 K matches well with the value recorded at ambient pressure. Within this framework, the depression of T_c with pressure can be ascribed to a reduction of λ mainly due to a decrease in $N(E_F)$. In this respect, it is crucial to understand the linear relation between the bulk T_c and $N(E_F)$, especially considering that this seems to also be the case for the well-known non-BCS superconductors Sr_2RuO_4 and UPt_3 [29]. It is noteworthy that the A magnitude of Nb_3Sn is well comparable to that of Sr_2RuO_4, and in the latter case, the simultaneous decrease of T_c and A under pressure is attributed to the weakening of electron-electron correlations [30].

On the other hand, Kataoka proposed that an electronic pairing mechanism based on Geĭlikman's model may apply to A15 superconductors [8,9]. According to Geĭlikman [39], in metals whose electronic structure consists of both light and heavy bands at the Fermi level, the Coulomb interaction between the light and heavy electrons causes an indirect attractive interaction. In practice, this attractive interaction can cooperate with the usual electron-phonon coupling to induce superconductivity in the light-electron system. A de Haas–van Alphen study [40] shows that Nb_3Sn has a multiband nature with the effective masses of the different bands ranging from 0.9 m_e to 5 m_e, where m_e is the free electron mass. As mentioned above, this type of band structure is the prerequisite

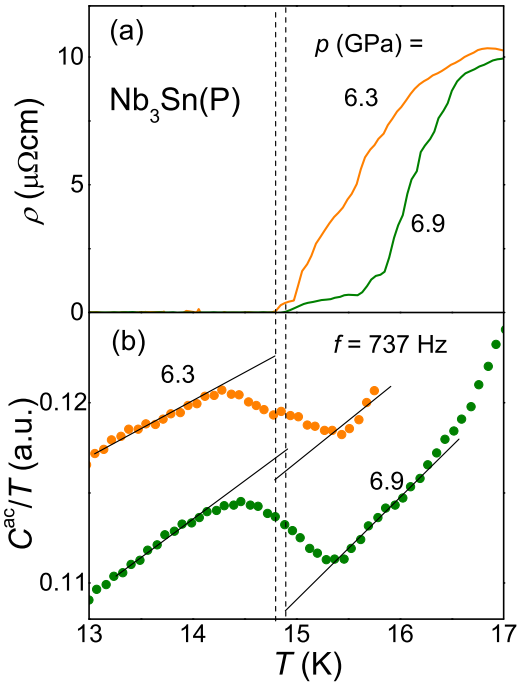

FIG. 6. Comparison of the resistivity and ac heat capacity at 6.3 and 6.9 GPa for Nb_3Sn(P). The heat capacity data were taken at a frequency of 737 Hz. The solid and dashed lines are a guide to the eyes.

for the Geĭlikman's mechanism. Thus it would be interesting to get a quantitative estimation of T_c as well as its pressure dependence in this picture.

IV. CONCLUSION

In summary, we have studied the resistivity of polycrystalline and single-crystalline Nb_3Sn samples under pressure up to 9.3 GPa. The T_c is more robust against pressure for the single-crystalline sample than for the polycrystalline one. For both samples, the normal-state resistivity follows a T^2 dependence, and the prefactor A of the T^2 law decreases with increasing pressure. Furthermore, the bulk T_c displays a linear dependence on $\sqrt{A}$, whose slope becomes larger with the increase of residual resistivity. These results highlight the importance of the electronic states at the Fermi level in determining T_c in Nb_3Sn under pressure, and call for a reexamination of their contribution to the superconducting pairing in this material.

ACKNOWLEDGMENT

We thank Enrico Giannini for performing SQUID measurements as well as fruitful discussions.

APPENDIX: COMPARISON OF THE RESISTIVITY AND AC HEAT CAPACITY UNDER PRESSURE

The pressure cells for both Nb_3Sn(S) and Nb_3Sn(P) were initially designed to measure both resistivity and ac heat capacity. However, due to the heater problem, pertinent heat-capacity results have been obtained only for Nb_3Sn(P) at 6.3 and 6.9 GPa. As shown in Fig. 6, in both cases, the completion of the resistive transition coincides with the midpoint of the heat capacity jump, which is taken as the bulk T_c in common practice when considering the entropy conservation [41]. Based on these results, we define T_c^{bulk} as the temperature corresponding to the completion of the resistive transition for all the other pressures.

[1] B. T. Matthias, T. H. Geballe, S. Geller, and E. Corenzwit, Phys. Rev. **95**, 1435 (1954).
[2] A. Godeke, Supercond. Sci. Technol. **19**, R68 (2006).
[3] G. R. Stewart, Physica C **514**, 28 (2015).
[4] T. Miyazaki, Y. Murakami, T. Hase, M. Shimada, K. Itoh, T. Kiyoshi, T. Takeuchi, K. Inoue, and H. Wada, IEEE Trans. Appl. Supercond. **9**, 2505 (1999).
[5] N. Mitchell, P. Bauer, D. Bessette, A. Devred, R. Gallix, C. Jong, J. Knaster, P. Libeyre, B. Lim, A. Sahu, and F. Simon, Fusion Eng. Design **84**, 113 (2009).
[6] A. Ballarino and L. Bottura, IEEE Trans. Appl. Supercond. **25**, 1 (2015).
[7] C. Paduani, Solid State Commun. **149**, 1269 (2009).
[8] M. Kataoka, J. Phys. Soc. Jpn. **54**, 29 (1985).
[9] M. Kataoka, J. Phys. C: Solid State Phys. **19**, 2939 (1986).
[10] D. F. Valentinis, C. Berthod, B. Bordini, and L. Rossi, Supercond. Sci. Technol. **27**, 025008 (2014).
[11] C. W. Chu, Phys. Rev. Lett. **33**, 1283 (1974).
[12] C. W. Chu, in *High-Pressure and Low-Temperature Physics*, edited by C. W. Chu and J. A. Woollam (Plenum, New York, 1978), p. 359.
[13] J. Labbe, Phys. Rev. **172**, 451 (1968).
[14] K. C. Lim, J. D. Thompson, and G. W. Webb, Phys. Rev. B **27**, 2781 (1983).
[15] G. W. Webb, Z. Fisk, J. J. Engelhardt, and S. D. Bader, Phys. Rev. B **15**, 2624 (1977).
[16] T. Spina, Ph.D. Thesis, Universite de Geneve, 2015, https://archive-ouverte.unige.ch/unige:74471.
[17] D. Jaccard, E. Vargoz, K. Alami-Yadri, and H. Wilhelm, Rev. High Pressure Sci. Technol. **7**, 412 (1998).
[18] H. Wiesmann, M. Gurvitch, H. Lutz, A. Ghosh, B. Schwarz, M. Strongin, P. B. Allen, and J. W. Halley, Phys. Rev. Lett. **38**, 782 (1977).
[19] R. Flükiger, D. Uglietti, C. Senatore, and F. Buta, Cryogenics **48**, 293 (2008).
[20] In these panels, the power-law exponent $n = 2$ is stable within an accuracy better than 0.2%.
[21] S. Tanaka, Handoko, A. Miyake, T. Kagayama, K. Shimizu, A. E. Böhmer, P. Burger, F. Hardy, C. Meingast, H. Tsutsumi, and Y. Ōnuki, J. Phys. Soc. Jpn. **81**, SB026 (2012).
[22] T. F. Smith, J. Low Temp. Phys. **6**, 171 (1972).
[23] A. Demuer, A. T. Holmes, and D. Jaccard, J. Phys.: Condens. Matter **14**, L529 (2002).
[24] M. Gurvitch, A. K. Ghosh, H. Lutz, and M. Strongin, Phys. Rev. B **22**, 128 (1980).
[25] R. Caton and R. Viswanathan, Phys. Rev. B **25**, 179 (1982).
[26] M. J. Rice, Phys. Rev. Lett. **20**, 1439 (1968).
[27] L. Qiao and X. J. Zheng, J. Appl. Phys. **112**, 113909 (2012).
[28] L. Qiao, L. Yang, and J. Song, Cryogenics **69**, 58 (2015).
[29] M. Núñez-Regueiro, G. Garbarino, and M. D. Núñez-Regueiro, J. Phys.: Conf. Ser. **400**, 022085 (2012).
[30] D. Forsythe, S. R. Julian, C. Bergemann, E. Pugh, M. J. Steiner, P. L. Alireza, G. J. McMullan, F. Nakamura, R. K. W. Haselwimmer, I. R. Walker, S. S. Saxena, G. G. Lonzarich, A. P. Mackenzie, Z. Q. Mao, and Y. Maeno, Phys. Rev. Lett. **89**, 166402 (2002).
[31] J. O. Willis, J. D. Thompson, Z. Fisk, A. de Visser, J. J. M. Franse, and A. Menovsky, Phys. Rev. B **31**, 1654(R) (1985).
[32] J. D. Thompson, M. W. McElfresh, J. O. Willis, Z. Fisk, J. L. Smith, and M. B. Maple, Phys. Rev. B **35**, 48 (1987).
[33] M. Núñez Regueiro, M. Jaime, M. A. Alario Franco, J.-J. Capponi, C. Chaillout, J.-L. Tholence, A. Sulpice, and P. Lejay, Physica C **235-240**, 2093 (1994).
[34] R. Falconi, A. Durán, M. Núñez-Regueiro, and R. Escudero, Phys. Status Solidi A **208**, 2159 (2011).
[35] A. K. Ghosh, M. Gurvitch, H. Wiesmann, and M. Strongin, Phys. Rev. B **18**, 6116 (1978).

[36] H. Wiesmann, M. Gurvitch, A. K. Ghosh, H. Lutz, O. F. Kammerer, and M. Strongin, Phys. Rev. B **17**, 122 (1978).
[37] W. L. McMillan, Phys. Rev. **167**, 331 (1968).
[38] H. M. Tütüncü, G. P. Srivastava, S. Bağci, and S. Duman, Phys. Rev. B **74**, 212506 (2006).
[39] B. T. Geĭlikman, Soviet Phys. JETP **21**, 796 (1965).
[40] N. Harrison, S. M. Hayden, P. Meeson, M. Springford, P. J. van der Wel, and A. A. Menovsky, Phys. Rev. B **50**, 4208 (1994).
[41] N. Tateiwa, Y. Haga, T. D. Matsuda, S. Ikeda, T. Yasuda, T. Takeuchi, R. Settai, and Y. Ōnuki, J. Phys. Soc. Jpn. **74**, 1903 (2005).